

# Porous Titanium Associated with CaP Coating: *In Vivo* and *In Vitro* Osteogenic Performance

Luana Marotta Reis de Vasconcellos<sup>a</sup>, Rodrigo Dias Nascimento<sup>b\*</sup>, Carlos Alberto Alves Cairo<sup>c</sup>,

Daniel de Oliveira Leite<sup>a</sup>, Evelyn Luzia de Souza Santos<sup>a</sup>, Gabriela Esteves Campos<sup>a</sup>,

Renata Falchete do Prado<sup>a</sup>, Maria Aparecida Neves Jardim<sup>b</sup>, Luis Gustavo Oliveira de Vasconcellos<sup>d</sup>,

Yasmin Rodarte Carvalho<sup>a</sup>

<sup>a</sup>Instituto de Ciência e Tecnologia de São José dos Campos, Departamento de Biociências e Diagnóstico Oral, Universidade Estadual Paulista - UNESP, São José dos Campos, SP, Brazil

<sup>b</sup>Instituto de Ciência e Tecnologia de São José dos Campos, Departamento de Diagnóstico e Cirurgia, Universidade Estadual Paulista - UNESP, São José dos Campos, SP, Brazil

<sup>c</sup>Instituto de Divisão de Materiais, Ar e Espaço, CTA, São José dos Campos, SP, Brazil

<sup>d</sup>Instituto de Ciência e Tecnologia de São José dos Campos, Departamento de Materiais Odontológicos e Prótese, Universidade Estadual Paulista - UNESP, São José dos Campos, SP, Brazil

Received: June 06, 2017; Revised: September 26, 2017; Accepted: November 19, 2017

This *in vitro* and *in vivo* study compared different topographies of Ti samples (dense, porosity of 30% and 40%) with or not CaP coating, prepared by powder metallurgy. Osteogenic cells from newborn rat calvaria were plated onto the samples and cell adhesion (24 hours), alkaline phosphatase activity (7 and 10 days) and mineralization nodules (14 days) were assessed. Sixteen rabbits were used for *in vivo* study. Each animal received three non-treated and three treated implants in the right or left tibia, respectively. Histometric evaluation of bone-implant contact (BIC) were assessed at 1, 2, 4 and 8 weeks. Metallographic analysis revealed porosities of 30% and 40%, with pore size ranging from 250 to 350  $\mu\text{m}$ . Cell adhesion test and ALP revealed similar cell behavior, independently of topography and CaP coating ( $P > 0.05\%$ ). However, CaP coating combined with porosity of 40% influenced positively the mineralized matrix formation ( $P < 0.05\%$ ). CaP-coated implants showed higher BIC than non-CaP implants and BIC was different between the short (1 and 2 weeks) and long (4 and 8 weeks) healing periods ( $P < 0.05\%$ ). The results suggest that CaP coating combined with 40% porosity implants allowed greater osteogenesis *in vitro* and increased BIC *in vivo*.

**Keywords:** bone in-growth, CaP coating, porous titanium, ALP, surface-cell adhesion.

## 1 Introduction

Porous, three-dimensional titanium materials have been used for many years in different clinical and medical applications as an option to enhance osseointegration and to induce greater bone-implant contact at short time<sup>1-5</sup>. In general, porous surfaces improve bone regeneration performance and implant fixation<sup>6-8</sup>. Specifically, the porous titanium can be an effective alternative material for biomedical application, such as sub-antral bone augmentation for dental implantation, reconstructive operations in maxillary sinus<sup>9</sup>, inter-body devices for spinal fusion<sup>4</sup>, regeneration of critical bone defects<sup>10</sup> and in patients with bone metabolism changes<sup>11,12</sup>. Another use for porous surfaces would involve bio-functionalization to achieve multi-functional biomaterials and load antimicrobial agents<sup>13</sup>. It is believed that most of these results are obtained because this surface provides optimal surface micro-relief, thus ensuring effective neo-vascularization during formation of new bone tissue<sup>9</sup>.

Additionally, previous *in vitro* studies reported that porous surfaces also provide good conditions for adhesion, expansion and migration of osteogenic cells<sup>14,15</sup>, increasing significantly the expression of bone proteins<sup>15,16</sup>. High porosity provides more space for bone in-growth and mechanical interlocking due to more surface area for implant-bone contact, enhancing the strength of interface and anchoring the implant to the surrounding bone<sup>6,17,18</sup>. All these factors prevent loosening of the implant and help to retain the dynamic strength of the implant.

Great attention has been paid to metallurgical techniques as they can produce samples mimicking natural bone and whose morphology is owned to their uniqueness, complexity and diversity<sup>19-22</sup>. Porous metal structure with inter-connective pores resembling the trabecular bone can be produced by a few techniques, and the powder metallurgy technique is widely used for this purpose due to its simple methodology of execution, permitting the control of inter-connected porosity. Our group had previously shown that it is possible to control both distribution and size of the pores size by means of this

\*e-mail: [nascimentodr@yahoo.com.br](mailto:nascimentodr@yahoo.com.br)

technique, with promising *in vivo* results of bone in-growth being described<sup>6,11,23</sup>.

Nowadays, the material engineering has focused on materials, which not only mimic the structure of natural bone but also be a biomimetic tissue to assist in the healing process, thus they should be bioactive as well as bio-resorbable<sup>24</sup>. Although hydroxyapatite (HA) is one component of the natural bone, it can be synthetically produced by different methods such as the biomimetic treatment<sup>15,17</sup>. Synthetic HA has a mineral composition similar to that of human bone, being then a biocompatible, osteoconductive and bioactivity material which enhances new bone formation at the bone-implant interface<sup>25</sup>.

Considering that porous titanium is an optimal material for osseointegration<sup>1,2,4</sup>, the present study tested the hypothesis that highly porous pure Ti scaffolds with CaP coating are the best alternative material. In this context, we evaluated the influence of Ti scaffolds with different size pores, submitted or not to CaP coating, on the osteoblast behavior *in vitro* and bone in-growth *in vivo* by means of biomimetic treatment.

## 2 Material and Methods

### 2.1 Development of Porous Titanium Implants and Samples

Pure Ti cylindrical implants exhibiting porous surface (4 mm diameter x 6 mm long) and pure Ti disc samples (12 mm x 3 mm) were prepared with powder metallurgy (Fig. 1). The disc samples and cylindrical implants were prepared as described in our previous studies<sup>1,11</sup>. All the samples were prepared by using pure Ti powders, which were developed in the General Command of Aerospace Technology (CTA)

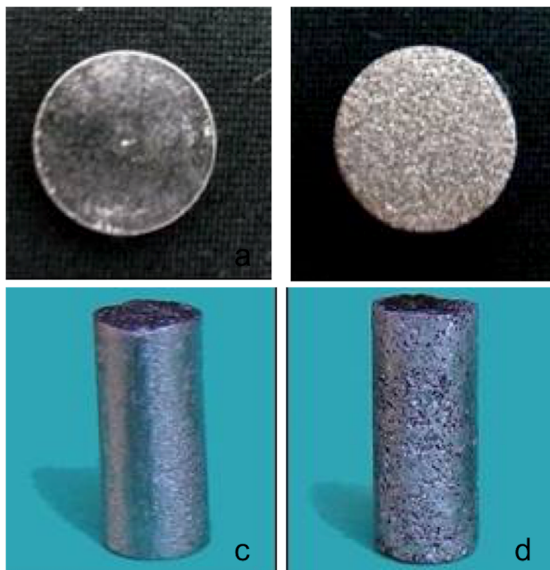


**Figure 1.** Macrostructure of the samples: a) dense Ti disc sample; b) porous Ti disc sample; c) dense Ti cylindrical implant; d) porous Ti cylindrical implant.

of the Institute of Air and Space (IAE), Division of Material (AMR), Brazil (purity  $\geq 99.5\%$ , particle size  $\leq 8 \mu\text{m}$ ) by means of hydrogenation and de-hydrogenation (HDDH). To fabricate porous structures, an organic additive (urea) with particle size ranging from 250 to 350  $\mu\text{m}$  was used as space holder. The weight ratio of Ti powder to space-holder was calculated by controlling the quantity of spacer particles in order to obtain defined porosities of 30 and 40% in the sintered samples. Dense implants and dense samples were produced by the same way, but without mixing urea as they were used as control.

### 2.2 CaP Coating

Half of the implants and samples were submitted to CaP coating by means of biomimetic treatment (BT) as follows. They received an alkaline treatment with several aqueous solutions of varying NaOH concentrations at 130°C in a vertical autoclave during 60 minutes for reaction time. Next, they were heated at 200 °C for 60 minutes in a tubular furnace (EDG 3P-S-1800, São Carlos, SP, Brazil) and subsequently cooled at room temperature inside the furnace. The substrate was soaked in simulated body fluid (SBF) with pH greater than 7.0 at 37°C for two weeks, and the SBF solution was replaced every two days before preparation according to the following ion concentrations: ( $\text{Na}^+$ ) = 142.00mM, ( $\text{K}^+$ ) = 5.00mM, ( $\text{Mg}^{2+}$ ) = 1.50mM, ( $\text{Ca}^{2+}$ ) = 2.50mM, ( $\text{Cl}^-$ ) = 147.80mM, ( $\text{HCO}_3^-$ ) = 4.20mM, ( $\text{HPO}_4^{2-}$ ) = 41:00mM and ( $\text{SO}_4^{2-}$ ) = 0.05mM.

By controlling the quantity and size of the spacer particles, we fabricated two different porous surfaces. Next, each group was subdivided according to whether or not they were submitted to CaP coating: Group 1, dense; Group 2, porosity of 30%; Group 3, porosity of 40%; Group 4, 5 and 6 with G1, G2 and G3 submitted to CaP coating, respectively. All the samples were sterilized by using gamma radiation at 20 kGy before *in vitro* and *in vivo* analyses.

### 2.3 Surface Characterization

The surface of five implants of each group was evaluated by metallographic analysis with SEM (LEO 435 VPI, Montreal, QC, Canada) at 100x magnification to verify pore morphology and interconnection, including topography of the porous structure. The *Image Tool* software (version 3.0 for Windows) was used to analyze area ( $\mu\text{m}^2$ ) and quantity (%) of pores. The implants were divided into 5 sections, and 3 images of each section were captured, totaling 15 images of each sample and of each implant. Additionally, they were submitted to analysis with energy dispersion spectrophotometry (EDS) (Oxford model - 7059) and Raman spectroscopy (Renishaw, 2000 model). In the EDS analysis three spots were selected in each sample in order to ascertain the elements present on their surface. Following to characterization of CaP coating as hydroxyapatite, the Raman spectroscopy equipped with argon laser with 514.5

nm wave length and spectrometer calibrated using silicon sample (Si) with characteristic peak at  $520\text{cm}^{-1}$  was used.

#### 2.4 Cell-Culture Isolation and Primary Culture of Osteogenic Cells

All animal procedures were performed in accordance with guidelines of the Research Ethics Committee of the São José dos Campos School of Dentistry (UNESP) (027/2008-PA/CEP). Cells from newborn (2-4 days) Wistar rat calvaria were harvested by using the enzymatic digestion process as previously described<sup>26</sup>. The cells were plated onto the samples in 24-well polystyrene plates and cultured as described previously<sup>14</sup>. Five samples from each group were used and all the assays were performed in triplicate, which were representative of three distinct primary cultures. All tests were developed in accordance with ISO-10993-5.

For evaluation of cell adhesion, cells were cultured on each sample for 24 hours. The proportion of cell growth was calculated from a baseline of 100% cells at the start of culture, and cell adhesion was expressed as a percentage of the number of plated cells. The method releasing thymolphthalein monophosphate (Labtest Diagnóstica, Belo Horizonte, Brazil) was used in accordance with the manufacturer's recommendations to determine ALP. Absorbance was measured in a UV 1203 spectrophotometer operating at 590 nm after 30 minutes. The results were expressed as ALP  $\mu\text{mol}$  thymolphthalein/min/mL. After 14 days in culture, the mineralized bone-like nodule formation was observed through staining with 2% Alizarin red S at pH of 4.2 and  $37^\circ\text{C}$  for 15 minutes. Reading was performed at 405 nm in a spectrophotometer, and the values were expressed as optical density. All tests were performed as previously described<sup>14</sup>.

#### 2.5 Animals and Surgical Procedure

A total of 16 male New Zealand albino rabbits aged 6 months old and weighing around 4.0 kg, were used in this study. This study was approved by the Ethics Research committee of the Sao Jose dos Campos School of Dentistry of Sao Jose dos Campos, UNESP (017/2010-PA/CEP).

The rabbits underwent bilateral surgery and received a total of 6 porous titanium implants in their cortical bone bed of the proximal left and right tibias as follows: 3 implants in the right tibia of G1, G2, G3 and 3 implants in the left tibia of G4, G5, G6. The insertion of implants was performed as described in our previous study<sup>11</sup>. The rabbits were euthanized at 1, 2, 4 and 8 weeks after implantation ( $n = 4$  rabbits for each experimental period).

#### 2.6 Histological and Histomorphometric Examination

Following euthanasia, four rabbits were submitted to histological and histomorphometric examination. The implantation area was sectioned and the tibial segments were immediately fixed with 10% formalin, dehydrated in

a graded alcohol series and embedded in methylmetacrylate. The fragments were histologically and histomorphometrically analyzed according to procedure described in our previous studies<sup>11,23</sup>. After processing, the sections had a final thickness of  $\sim 60\ \mu\text{m}$  and were stained with toluidine blue for histomorphometric analysis using light microscope (Axioplan 2, Carl Zeiss, Germany) combined with a digital camera (Sony, DSC-S85, Cyber-shot).

Three sections were obtained from each implant of the four different rabbits of each group. A blinded investigator, who used 2 different images representing medial and distal faces of each section of the bone-implant interface, evaluated osseointegration. Thus, eight fields of each implant were digitized (100x). New bone formation and bone in-growth into the interior of the pores were calculated by using Image J software (NIH). The interfaces were also evaluated with SEM.

#### 2.7 Statistics

Statistical analysis of cell adhesion and ALP data was performed by using parametric or non-parametric tests for independent data (Kruskal-Wallis and ANOVA, respectively), followed by a multiple comparison test (Tukey's and Dunn's tests, respectively) ( $P < 0.05$ ).

All quantitative data were expressed as mean  $\pm$  standard deviation (SD) values. Histomorphometric results of bone in-growth depth were statistically analyzed by using randomized block design ANOVA with *post-hoc* Tukey's test ( $P < 0.05$ ) to determine differences between the implant conditions.

### 3 Results

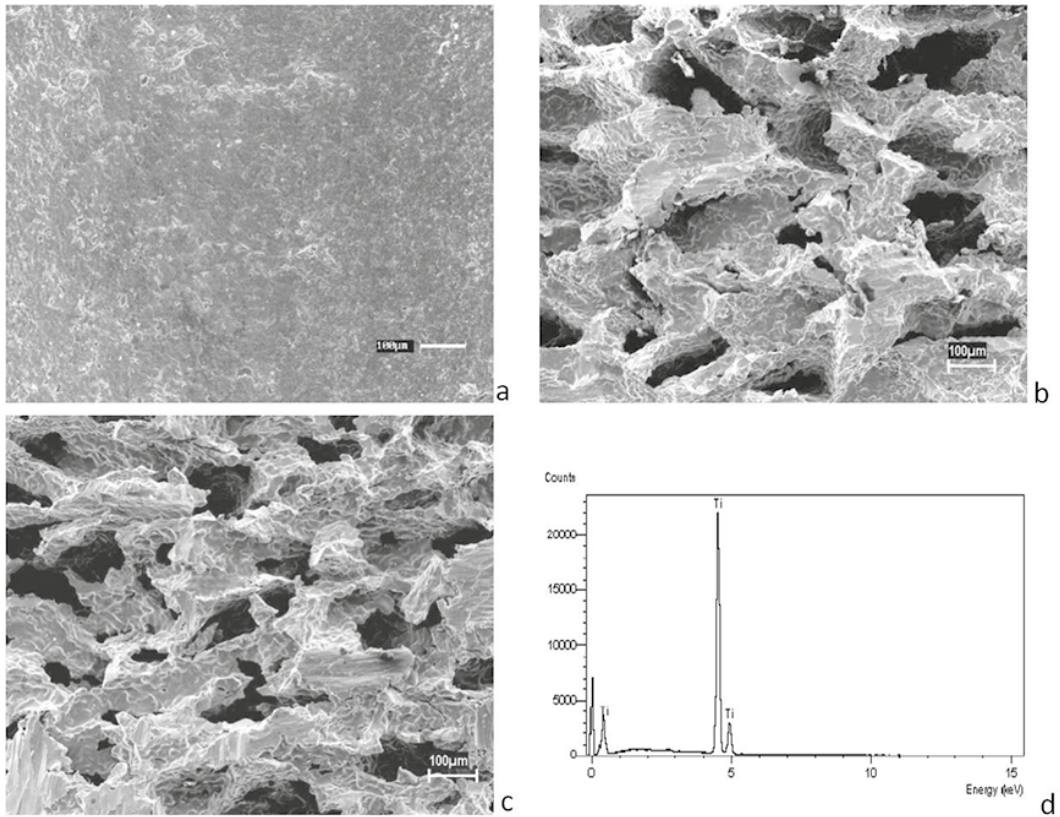
#### 3.1 Discs Samples and Implant Characterization

Figure 2 shows morphology of the dense and both porous samples and the results of EDS analysis, confirming that the main element of the material was titanium.

Figure 3 shows the dense and both porous samples submitted to CaP coating and the results of EDS analysis exhibiting the characteristic peak energy of elements calcium (Ca), phosphorus (P) and oxygen (O) and titanium (Ti).

The porous structure in both disc samples and implants exhibited interconnected pores. Metallographic analysis revealed pores with mean diameter of  $300\ \mu\text{m} \pm 8.25$  and structures with porosities of 30% and 40%, which was achieved by controlling the quantity of spacer particles (urea).

It was observed pores distribution in all sample. Figures 2 and 3 show images of irregular pores with small and large sizes as previously described<sup>27</sup>. Larger pores are suitable for transportation of body fluids and bone in-growth, whereas the others being the result of the sintering process. In dense structures, both samples and implants exhibited some few small, isolated pores as a result of volume shrinkage during the sintering process of the titanium powders.



**Figure 2.** SEM image of pure Ti: a) dense sample; b) 30% porous sample; c) 40% porous sample; d) EDS results.

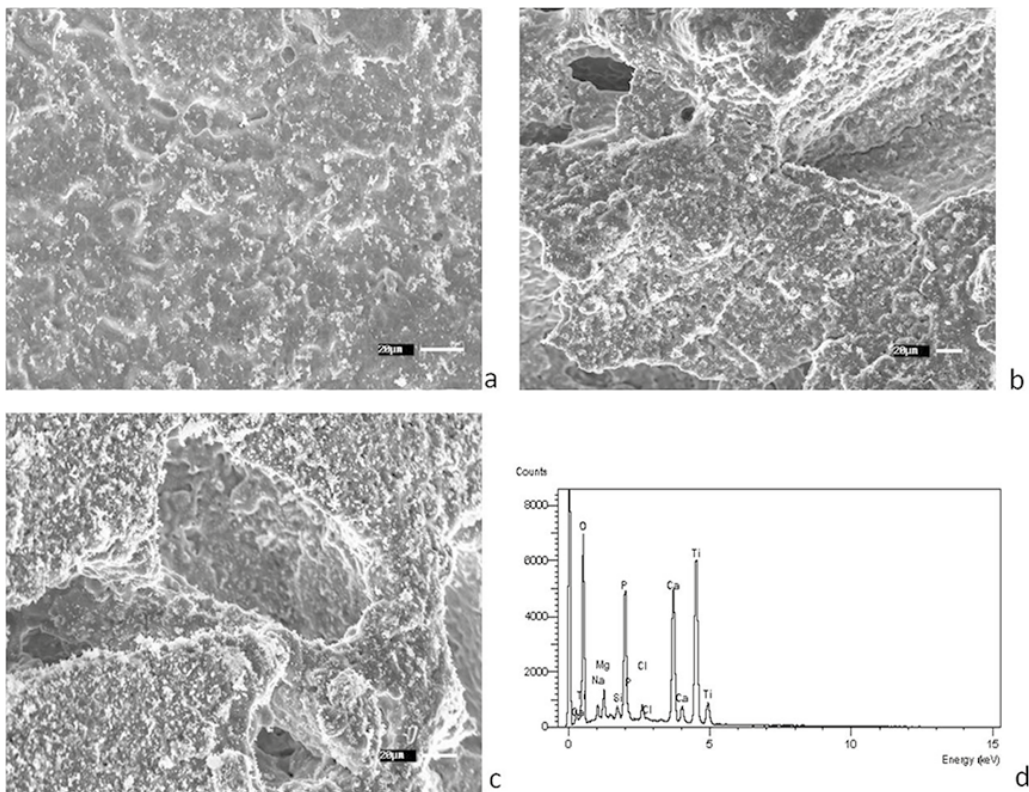


**Figure 3.** SEM image pure Ti submitted to CaP coating Ca: a) dense sample; b) 30% porous sample; c) 40% porous sample; d) EDS results.

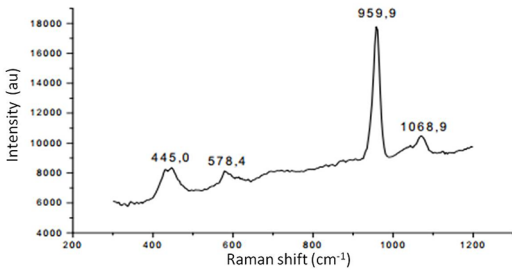


**Figure 4.** Raman spectra of hydroxyapatite before CaP coating (A). Broad bands are due to the overlapping of the optical window signal.

As shown in Figure 4, it was possible to observe the high magnitude of the hydroxyapatite peak, approximately to 960  $\text{cm}^{-1}$ , corresponding to the phosphate functional group ( $\text{PO}_3^{-4}$ ), according previously results<sup>28</sup>.

### 3.2 *In Vitro* Assessment

The groups showed similar values of cell adhesion ( $P>0.05$ ), with surface topography or presence of CaP coating having no significant impact on cell attachment. Moreover, there was no difference between the groups although the

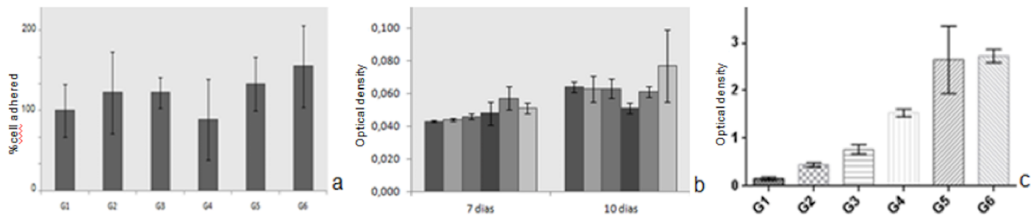


**Figure 5.** Effect of sample on cell adhesion (a), ALP (b), mineralized matrix (c).

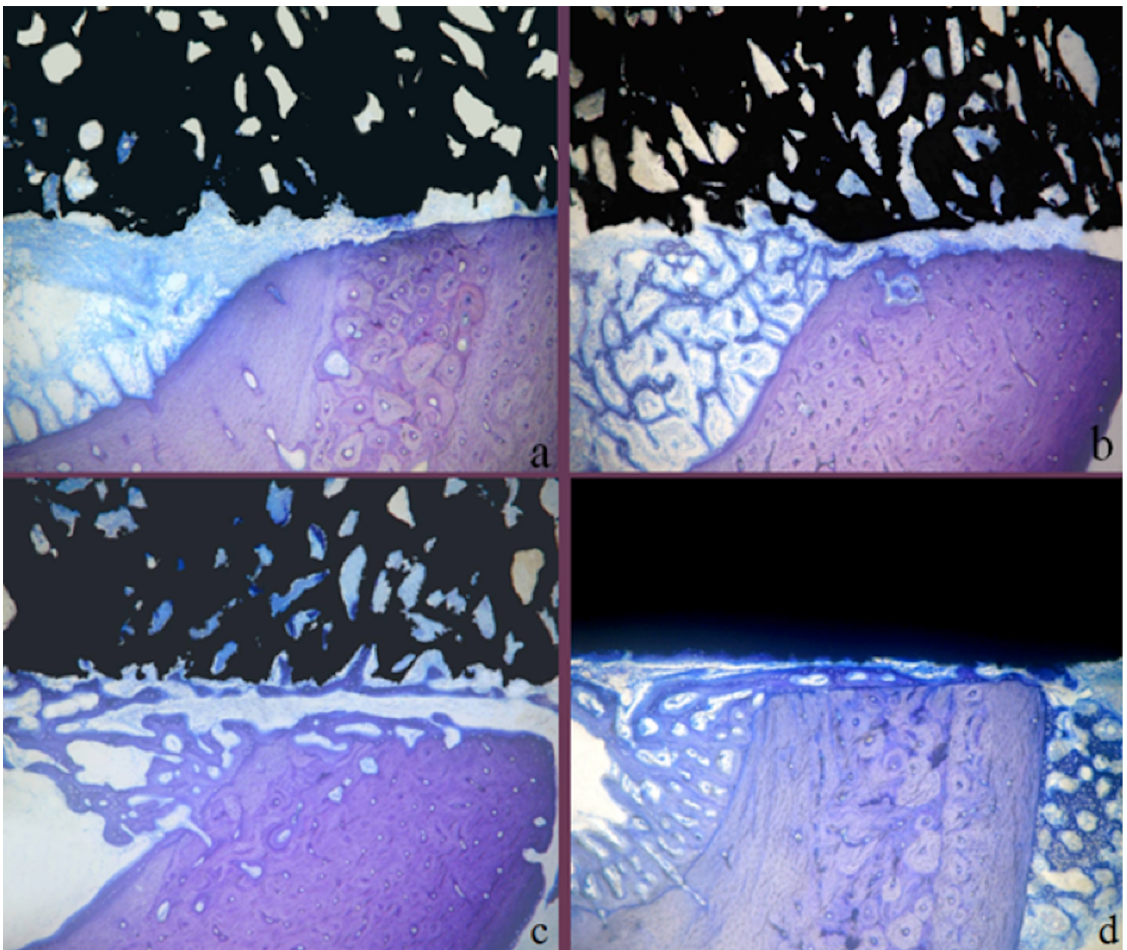


**Figure 6.** Initial periods at 1 week: a) panoramic vision at bone-implant interface without CaP coating (original magnification 50x); b) panoramic vision at bone-implant interface with CaP coating (original magnification 50x); at 2 weeks: c) panoramic vision at bone-implant interface without CaP coating (original magnification 50x); d) panoramic vision at bone-implant interface with CaP coating (original magnification 50x).

40% porosity surface submitted to CaP coating exhibited greater cell adhesion (Fig. 5a).

ALP activity (Fig. 5b) was found to be similar at 7 and 10 days ( $P>0.05$ ), with values between the groups showing no statistical difference ( $P>0.05$ ). However, it is important to emphasize that Group 6 had the higher value of ALP, similar to that of cell adhesion.

After 14 days in culture, bone-like nodule formations in all Ti discs were observed (Fig. 5c). Bone-like nodule formation was affected by the Ti chemical composition, being greater in G6 ( $P<0.05$ ).

### 3.3 Histological Examination

No fibrous tissue was observed at the interface, regardless of either sample type or sacrifice period. New bone formation towards the implant and inwards the pores was also observed, filling partially or fully them on an increasing basis over time, regardless of the euthanasia period. This new bone consisted of trabecular bone presenting lamellar arrangement

and different-sized medullary spaces. A distinct border was observed between newly formed bone and pre-existing bone, especially in rabbits sacrificed at 4 weeks.

At the early periods of osseointegration, there was formation of trabecular bone surrounding the implant surface in the groups submitted to biomimetic treatment, with proliferation of immature osseous trabeculae at the medullary region, which was not observed in the samples not submitted to biomimetic treatment (Fig. 6).

At 4 and 8 weeks, new bone formation surrounding the samples and great interconnection between bone and implant were observed compared to the early periods (Fig. 7). This tissue was found to be more mature and organized than that of earlier periods. In the porous samples, one can observe a bone tissue growth inwards the pores, sometimes resulting in partial or full filling (Fig. 8). There was also a qualitative similarity in the structural pattern of new bone formation, regardless of the type of topography and presence of coverage.

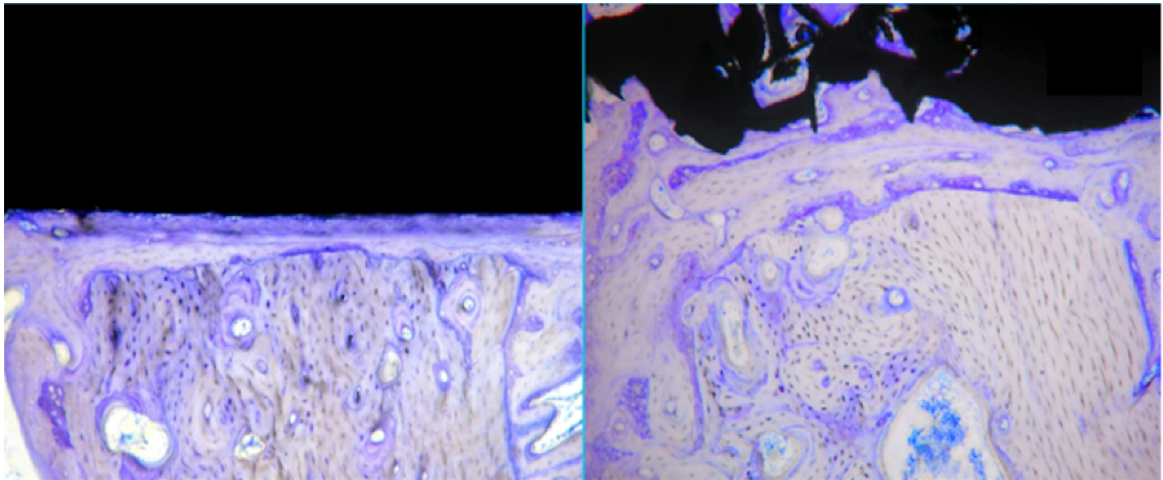


**Figure 7.** Bone-implant interface at 8 weeks: a) osseointegration and new bone formation at the interface of dense implants (original magnification 10x); b) bone in-growth into a porous surface titanium sample (original magnification 10x).

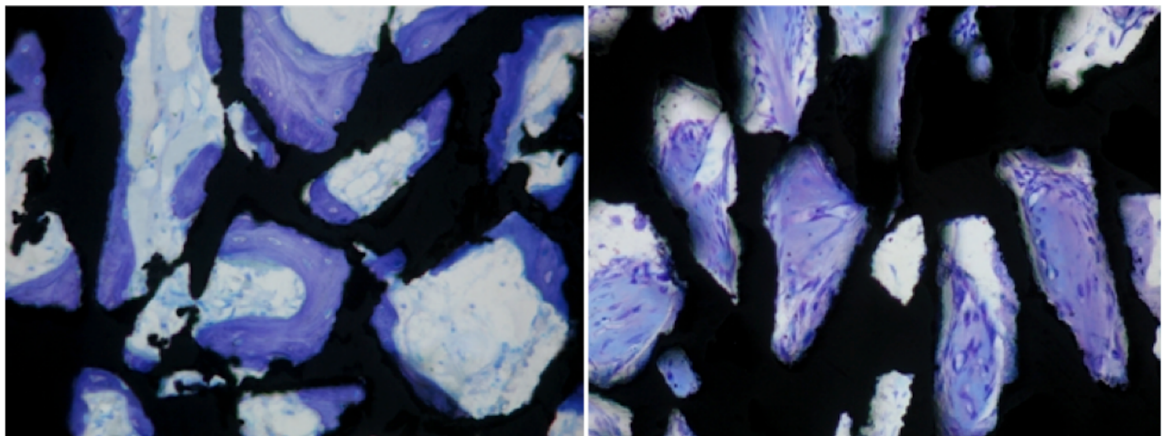


**Figure 8.** Bone in-growth into the pores: a) at 4 weeks showing partial filling, b) at 8 weeks showing increase of bone in-growth.

### 3.4 Histomorphometric Examination

The bone in-growth rates are presented in the graph below (Fig. 9). The average values regarding the percentage of new bone formation were not significantly different at 4 and 8 weeks compared to that at 1 and 2 weeks after implantation ( $P>0.05$ ). However, there was a statistically significant difference ( $P<0.05$ ) between short (1 and 2 weeks) and long periods (4 and 8 weeks).

Table 1, after statistical analysis with two-way ANOVA, shows that there were statistically significant differences between the implant types ( $P<0.05$ ). G1 (dense implant without CaP coating) presented the lowest amount of new bone, differing from other groups, whereas G6 (porous implant with 40% porosity and CaP coating) and G5 (porous implant with 30% porosity and CaP coating) showed the greatest amount of new bone, also differing from other groups. G3 and G2 presented no statistically significant difference between them ( $P>0.05$ ), but G3 differed from G4 and G2 showed similar results compared to G4. This may be explained because G3 presented the highest percentage of pores and G2 presented more new bone formation. This result suggests that enhancing the contact surface by increasing the percentage of pores is an alternative to improve bone cell proliferation.

The dense groups (G1 and G4) exhibited statistically significant difference ( $P<0.05$ ), suggesting that biomimetic coating influenced positively the new bone formation *in vivo*.

### 4. Discussion

Porous Ti is considered to be an ideal graft material in orthopedic and dental surgeries due to its similar spatial structures and mechanical properties to cancellous bone, although its bio-inert property demands modifications to improve the osseointegration capacity<sup>30</sup>. The modification of surface topography in association with CaP treatment has demonstrated promising results in the development of implants for biomedical applications<sup>31-34</sup>. Among the reasons justifying these results, there is the fact that bioactive covering of porous surfaces allows rapid osseointegration of the surrounding bone tissue as well as direct chemical linking between bone and implant<sup>35</sup>. Then, new surface has been continuously developed with the objective to be used in biomedical applications<sup>9,13,22,29,30</sup>.

Porous scaffolds have attracted considerable attention for applications in bone tissue engineering because their interconnected pores can provide a favorable environment for bone in-growth and osseointegration<sup>1,2,14,15,23</sup>. The ideal porous implants should provide sufficient porosity for cell migration and tissue in-growth by creating a good and appropriate way to remodel and guide regenerating tissue<sup>16</sup>. Amount, size, orientation and interconnectivity of the pores interfere positively with cell behavior. Studies have suggested that porous surface improves osseointegration because it provides a greater area at the implant-bone interface<sup>1-3,20,23,36</sup>.

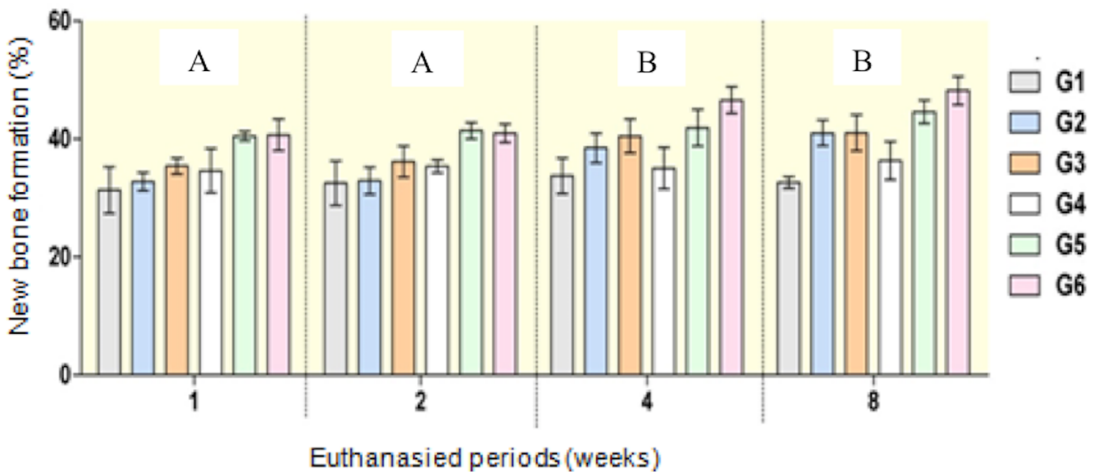


Figure 9. Graphics of media and standard deviation ( $\pm$ ) of neoformation bone in interface bone-implant.

Table 1. Sample x mean x non-homogeneous groups

Sample Group	Mean	Non-homogeneous groups		
G6	44,106	A		
G5	42,098	A		
G3	38,278		B	
G2	36,292		B	C
G4	35,332			C
G1	32,565			D

It is important highlight that there was an optimal percentage of porosity for bone in-growth to allow cell adhesion and proliferation in addition to transportation of body fluids into them. Porosity has been reported to range from 25 e 67%<sup>1,6</sup>, and in our study the samples had porosities of 30% and 40%, which produced satisfactory results *in vitro* and *in vivo*. Data indicate that scaffolds with lower porosity have less bone in-growth. Although increased porosity is preferential for new bone growth in Ti implants, it should be kept in mind that another consequence of increased porosity is a reduction in the mechanical properties of the implant. Thus, depending on the intended application, a balance between mechanical properties and biological performance should be established<sup>23</sup>.

Clinical practices and studies have shown that the mechanical mismatch between metallic implant and natural bone may lead to stress-shielding, and thus cause bone resorption and eventually failure of metallic implant fixation. Porous metallic structure can be used to overcome this drawback, which not only reduces mechanical mismatch but also achieves stable long-term fixation by promoting full bone in-growth<sup>16</sup>.

The titanium surface is not enough to induce bone formation in the early periods of healing. Therefore, chemical modifications on the implant surfaces by means of bioactive covering have also been proposed by researchers in order to improve biological properties involving the bone-implant interaction. The biomimetic treatment is a method using supersaturated solution to form a calcium phosphate layer (e.g. hydroxyapatite), making the implant's surface osseointegrative<sup>29,34,37</sup>. In order to assess the precipitation of calcium and phosphate ions, the samples were observed with EDS analysis in which peaks of these ions had been observed on a diffractogram, a finding also reported elsewhere<sup>34,37</sup>.

Cell behavior is closely related to the cell-material contact, thus events such as cell adhesion and spreading are steps which may influence proliferation and differentiation of cells<sup>14,38-41</sup>. The results of our study showed that there was influence of topography and surface covering on cell response. In the adhesion test, one can observe the presence of cell adhesion in all experimental groups, but this was greater in the group of treated porous samples. In the ALP evaluation, it was observed that there was differentiation of osteoblastic cells and higher metabolism in the group of treated porous samples as well. This result can be explained based on the differentiation process and synthesis activity of these cells, which are usually sensitive to the type of material being used<sup>14,15,41</sup>. The formation of mineralized matrix is considered an *in vitro* functional parameter, reflecting an advanced cell differentiation. In this study, the amount of mineralized matrix was greater in the group of treated porous samples.

Histomorphometric analysis in the present study showed that dense surface without treatment had a significantly less bone in-growth. This occurred as a consequence of the implant

structure, which was dense. In contrast, porous samples exhibited an increased area of bone formation, including inside the pores. These data suggest that new bone growth and bone conduction are definitely influenced by porosity as the new bone tissue fills the pores, thus increasing the bone-implant interface and consequently enhancing the mechanical interlocking and implant stability<sup>1,6,16,42</sup>.

Tissue response and new bone formation are complex biological phenomena and any change in the implant surface can influence them directly. Histological and histomorphometric analyses have demonstrated that the association between porous surface and chemical treatment resulted in more new bone formation in all experimental periods. We emphasize that it was possible to observe proliferation of osteoid tissue towards the implant at 1 week, suggesting greater osteoconductivity and rapid bone repair surrounding the implant in the samples with porous surface submitted to chemical-thermal treatments.

## 5. Conclusions

In view of the results found one can conclude that the powder metallurgy technique enables to control the quantity of pores and that a higher percentage of pores play a positive influence on cell behavior, a fact which could be demonstrated in *in vitro* tests. Moreover, it was also concluded that biomimetic treatment enhances early new bone formation by speeding up the osseointegration process; In this way, highly porous implants associated with bioactive coating have great potential for biomedical purposes.

## 6. Acknowledgment

This study was supported by research grant numbers 2005/03709-4 and 2007/08593-0 awarded by the State of São Paulo Research Foundation (FAPESP), Brazil.

## 7. References

1. Vasconcellos LMR, Oliveira MV, Graça MLA, Vasconcellos LGO, Carvalho YR, Cairo CAA. Porous titanium scaffolds produced by powder metallurgy for biomedical applications. *Materials Research*. 2008;11(3):275-280.
2. Wazen RM, Lefevre LP, Baril E, Nanci A. Initial evaluation of bone ingrowth into a novel porous titanium coating. *Journal of Biomedical Materials Research. Part B: Applied Biomaterials*. 2010;94B(1):64-71.
3. Bari E, Lefebvre LP, Hacking SA. Direct visualization and quantification of bone growth into porous titanium implants using micro computed tomography. *Journal of Materials Science: Materials in Medicine*. 2011;22(5):1321-1332.
4. Guyer RD, Abitbol JJ, Ohnmeiss DD, Yao C. Evaluating Osseointegration into a Deeply Porous Titanium Scaffold: A Biomechanical Comparison with PEEK and Allograft. *Spine (Phila Pa 1976)*. 2016;41(19):E1146-50.

5. Ong JL, Hoppe CA, Cardenas HL, Cavin R, Carnes DL, Sogal A, et al. Osteoblast precursor cell activity on HA surfaces of different treatments. *Journal of Biomedical Materials Research. Part A*. 1998;39(2):176-183.
6. Vasconcellos LMR, Oliveira MV, Graça MLA, Vasconcellos LGO, Cairo CAA, Carvalho YR. Design of dental implants, influence on the osteogenesis and fixation. *Journal of Materials Science: Materials in Medicine*. 2008;19(8):2851-2857.
7. Deporter DA, Watson PA, Pilliar RM, Melcher AH, Winslow J, Howley TP, et al. A histological assessment of the initial healing response adjacent to porous-surfaced, titanium alloy dental implants in dogs. *Journal of Dental Research*. 1986;65(8):1064-1070.
8. Pilliar RM, Deporter DA, Watson PA, Todescan R. The endopore implant-enhanced osseointegration with a sintered porous-surfaced design. *Oral Health*. 1998;88(7):61-64.
9. Sirak SV, Shchetinin EV, Sletov AA. Subantral augmentation with porous titanium in experiment and clinic. *Stomatologiya (Mosk)*. 2016;95(1):55-58.
10. Van der Stok J, Van der Jagt OP, Amin Yavari S, De Haas MF, Waarsing JH, Jahr H, et al. Selective laser melting-produced porous titanium scaffolds regenerate bone in critical size cortical bone defects. *Journal of Orthopaedic Research*. 2013;31(5):792-799.
11. Vasconcellos LM, Oliveira FN, Leite DO, Vasconcellos LG, Prado RF, Ramos CJ, et al. Novel production method of porous surface Ti samples for biomedical application. *Journal of Materials Science: Materials in Medicine*. 2012;23(2):357-364.
12. Guo Z, Iku S, Mu L, Wang Y, Shima T, Seki Y, et al. Implantation with new three-dimensional porous titanium web for treatment of parietal bone defect in rabbit. *Artificial Organs*. 2013;37(7):623-628.
13. Amin Yavari S, Loozen L, Paganelli FL, Bakhshandeh S, Liettaert K, de Groot J, et al. Antibacterial Behavior of Additively Manufactured Porous Titanium with Nanotubular Surface Releasing Silver Ions. *ACS Applied Materials & Interfaces*. 2016;8(27):17080-17089.
14. de Andrade DP, de Vasconcellos LM, Carvalho IC, Forte LF, de Souza Santos EL, Prado RF, et al. Titanium-35niobium alloy as a potential material for biomedical implants: In vitro study. *Materials Science and Engineering: C*. 2015;56:538-544. DOI: 10.1016/j.msec.2015.07.026
15. do Prado RF, Rabêlo SB, de Andrade DP, Nascimento RD, Henriques VA, Carvalho YR, et al. Porous titanium and Ti-35Nb alloy: effects on gene expression of osteoblastic cells derived from human alveolar bone. *Journal of Materials Science: Materials in Medicine*. 2015;26(11):259.
16. Choy MT, Tang CY, Chen L, Wong CT, Tsui CP. In vitro and in vivo performance of bioactive Ti6Al4V/TiC/HA implants fabricated by a rapid microwave sintering technique. *Materials Science and Engineering: C*. 2014;42:746-756.
17. do Prado RF, de Oliveira FS, Nascimento RD, de Vasconcellos LM, Carvalho YR, Cairo CA. Osteoblast response to porous titanium and biomimetic surface: In vitro analysis. *Materials Science and Engineering: C*. 2015;52:194-203.
18. Thelen S, Barthelat F, Brinson LC. Mechanics considerations for microporous titanium as an orthopedic implant material. *Journal of Biomedical Materials Research. Part A*. 2004;69(4):601-610.
19. An YB, Lee WH. Synthesis of porous titanium implants by environmental-electro-discharge-sintering process. *Materials Chemistry and Physics*. 2006;95(2-3):242-247.
20. Ryan G, Pandit A, Apatidis DP. Fabrication methods of porous metals for use in orthopaedic applications. *Biomaterials*. 2006;27(13):2651-2670.
21. Nugroho AW, Leadbeater G, Davies IJ. Processing of a porous titanium alloy from elemental powders using a solid state isothermal foaming technique. *Journal of Materials Science: Materials in Medicine*. 2010;21(12):3103-3107.
22. Chen JY, Yang CY, Chen PY. Synthesis of hierarchically porous structured CaCO<sub>3</sub> and TiO<sub>2</sub> replicas by sol-gel method using lotus root as template. *Materials Science and Engineering: C*. 2016;67:85-97.
23. Vasconcellos LMR, Leite DD, Nascimento FO, Vasconcellos LGO, Graça MLA, Carvalho YR, et al. Porous titanium for biomedical applications: an experimental study on rabbits. *Medicina Oral, Patología Oral y Cirugía Bucal*. 2010;15(2):e407-412.
24. Wepener I, Richter W, van Papendorp D, Joubert AM. In vitro osteoclast-like and osteoblast cells' response to electrospun calcium phosphate biphasic candidate scaffolds for bone tissue engineering. *Journal of Materials Science: Materials in Medicine*. 2012;23(12):3029-3040.
25. Rodrigues CV, Serricella P, Linhares AB, Guerdes RM, Borojevic R, Rossi MA, et al. Characterization of a bovine collagen hydroxyapatite composite scaffold for bone tissue engineering. *Biomaterials*. 2003;24(27):4987-4997.
26. Nanci A, Zalzal S, Gotoh Y, McKee MD. Ultrastructural characterization and immunolocalization of osteopontin in rat calvarial osteoblast primary cultures. *Microscopy Research & Technique*. 1996;33(2):214-231.
27. Čapek J, Vojtěch D. Properties of porous magnesium prepared by powder metallurgy. *Materials Science and Engineering: C*. 2013;33(1):564-569.
28. Penel G, Delfosse C, Descamps M, Leroy G. Composition of bone and apatitic biomaterials as revealed by intravital Raman microspectroscopy. *Bone*. 2005;36(5):893-901.
29. Wang Q, Qiao Y, Cheng M, Jiang G, He G, Chen Y, et al. Tantalum implanted entangled porous titanium promotes surface osseointegration and bone ingrowth. *Scientific Reports*. 2016;6:26248.
30. Yin B, Ma P, Chen J, Wang H, Wu G, Li B, et al. Hybrid Macro-Porous Titanium Ornamented by Degradable 3D Gel/nHA Micro-Scaffolds for Bone Tissue Regeneration. *International Journal of Molecular Sciences*. 2016;17(4):575.
31. Nishiguchi S, Kato H, Fujita H, Oka M, Kim HM, Kokubo T, et al. Titanium metals form direct bonding to bone after alkali and heat treatments. *Biomaterials*. 2001;22(18):2525-2533.
32. Li JP, Li SH, Van Blitterwijk CA, de Groot K. Cancellous bone from porous Ti6Al4V by multiple coating technique. *Journal of Materials Science: Materials in Medicine*. 2006;17(2):179-185.

33. Otsuki B, Takemoto M, Fujibayashi S, Neo M, Kokubo T, Nakamura T. Pore throat size and connectivity determine bone and tissue ingrowth into porous implants: three-dimensional micro-CT based structural analyses of porous bioactive titanium implants. *Biomaterials*. 2006;27(35):5892-5900.
34. Escada AL, Machado JP, Schneider SG, Rezende MC, Claro AP. Biomimetic calcium phosphate coating on Ti-7.5Mo alloy for dental application. *Journal of Materials Science: Materials in Medicine*. 2011;22(11):2457-2465.
35. Vasudev DV, Ricci JL, Sabatino C, Li P, Parsons JR. In vivo evaluation of a biomimetic apatite coating grown on titanium surfaces. *Journal of Biomedical Materials Research. Part A*. 2004;69(4):629-636.
36. Faria PEP, Carvalho AL, Felipucci DNB, Wen C, Sennerby L, Salata LA. Bone formation following implantation of titanium sponge rods into humeral osteotomies in dogs: a histological and histometrical study. *Clinical Implant Dentistry and Related Research*. 2010;12(1):72-79.
37. Capellato P, Escada AL, Popat KC, Claro AP. Interaction between mesenchymal stem cells and Ti-30Ta alloy after surface treatment. *Journal of Biomedical Materials Research. Part A*. 2014;102(7):2147-2156.
38. Bowers KT, Keller JC, Randolph BA, Wick DG, Michaels CM. Optimization of surface micromorphology for enhanced osteoblast responses in vitro. *International Journal of Oral & Maxillofacial Implants*. 1992;7(3):302-310.
39. Anselme K, Biggerelle M. Topography effects of pure titanium substrates on human osteoblast long-term adhesion. *Acta Biomaterialia*. 2005;1(2):211-222.
40. Rosa AL, Beloti MM. Effect of cpTi surface roughness on human bone marrow cell attachment, proliferation, and differentiation. *Brazilian Dental Journal*. 2003;14(1):16-21.
41. Sista S, Wen C, Hodgson PD, Pande G. The influence of surface energy of titanium-zirconium alloy on osteoblast cell functions in vitro. *Journal of Biomedical Materials Research. Part A*. 2011;97(1):27-36.
42. Yang GL, He FM, Hu JA, Wang XX, Zhao SF. Biomechanical comparison of biomimetically and electrochemically deposited hydroxyapatite-coated porous titanium implants. *Journal of Oral and Maxillofacial Surgery*. 2010;68(2):420-427.